Front and pulse solutions for the complex Ginzburg-Landau equation with higher-order terms

Huiping Tian,* Zhonghao Li,† Jinping Tian,‡ and Guosheng Zhou‡
Department of Electronics and Information Technology, Shanxi University, Taiyuan, Shanxi, 030006, People's Republic of China
(Received 26 January 2002; revised manuscript received 29 August 2002; published 10 December 2002)

We investigate one-dimensional complex Ginzburg-Landau equation with higher-order terms and discuss their influences on the multiplicity of solutions. An exact analytic front solution is presented. By stability analysis for the original partial differential equation, we derive its necessary stability condition for amplitude perturbations. This condition together with the exact front solution determine the region of parameter space where the uniformly translating front solution can exist. In addition, stable pulses, chaotic pulses, and attenuation pulses appear generally if the parameters are out of the range. Finally, applying these analysis into the optical transmission system numerically we find that the stable transmission of optical pulses can be achieved if the parameters are appropriately chosen.

DOI: 10.1103/PhysRevE.66.066204 PACS number(s): 05.45.Pq, 42.65.Sf, 42.81.Dp, 47.10.+g

I. INTRODUCTION

Problems in dynamics have fascinated physical scientists and mankind in general for thousands of years [1]. Coherent structures are an important element in the long-time dynamics of pattern forming systems and have attracted a great deal of attention in recent years [2]. Several kinds of coherent structures such as fronts, pulses, sources and sinks have been studied [2–4] and identified in many experiments, such as thermal convection [2], Taylor-Couette flow [5–7], parametric surface waves in fluids [8], plane Poiseuille flow [9], nonlinear light-wave propagation in fibers [10,11] and oscillatory chemical reactions [12]. The one-dimensional complex Ginzburg-Landau equation (CGLE) and its different modifications have been employed to describe these phenomena in laser physics [13], fluid dynamics [14] and nonlinear optics [15–18].

Spatially extended nonequilibrium systems often show coherent structures formed from the spatial juxtaposition of different types of solutions, particularly near subcritical bifurcations where the different solutions are individually stable [19]. Examples are moving fronts formed when a stable state invades an unstable one or fronts between stable states. Depending on parameter values these coherent structures are found to vary either periodically or chaotically in time, and to have spatial envelopes which may be stationary or uniformly moving, or may undergo chaotic motion. The comprehensive analytic and numerical studies of the one-dimensional CGLE near a subcritical bifurcation have been presented in Refs. [20–23].

Noting that all these analysis of the multiplicity of solutions were based on CGLE. But the CGLE with higher-order terms has less extensively been analyzed except that Desissler and Brand [24] have numerically investigated the effect of a nonlinear gradient term recently. However, they are worth investigating further as mentioned by Saarloos and Hobenberg [2], since the more general model is useful for understanding various experimental phenomena. Another useful example, from the standpoint of possible applications, is the optical pulse transmission line. The propagation of picosecond optical pulses in optical fibers is approximately governed by nonlinear Schrödinger equation (NLSE). When frequency- and intensity-dependent gain and loss have to be taken into account for a long distance communication, the governing equation should be replaced by cubic CGLE [5]. For intensive and short optical pulse in the subpicosecond or femtosecond regime, several new effects, such as third-order dispersion (TOD), self-steepening and self-frequency-shift (SFS) arising from stimulated Raman scattering, greatly influence their propagation properties [25]. When TOD is compensated, the equation to describe the propagation of ultrashort pulses will reduce to the CGLE with higher-order terms [2].

The objective of this work is to analyze the CGLE with the higher-order terms by using a particular exact analytic front solution as an ansatz and to understand the multiplicity of the front solution of this equation, and to elucidate the ensuing selection problem: which solution will be reached starting from specified initial conditions. We generalized ''linear and nonlinear marginal stability'' criteria to the general case with the help of the methods mentioned in Refs. [2,26]. Our main result is the discovery of an exact ''selected'' front solution which allows us to predict analytically whether a pulse or a front will be preferred, and in the latter case what the front velocity will be. Another result is that the pulse is always unstable to front generation in the parameter range where front is selected, while out of the range we can obtain stable pulses, chaotic pulses, and attenuation pulses by numerical simulation.

*Email address: tianhuip@mail.sxu.edu.cn. Fax: +86-0351-7011500.
†Corresponding author. Email address: lizhongh@mail.sxu.edu.cn Fax: +86-0351-7011500.
‡Fax: +86-0351-7011500.

II. THE MODEL AND THE EXACT FRONT SOLUTIONS

The generalized Ginzburg-Landau equation for the complex function $A(x,t)$ in one-dimension space has the following form [2]:

$$\partial_t A=(b_1+ic_1)\partial_x^2 A+f_1(|A|^2)A+\partial_x[f_2(|A|^2)A]+[\partial_x f_3(|A|^2)]A, \quad (1)$$

where b_1 and c_1 are real constants and the f_l are generally complex functions of the real argument $|A|^2$ with:

$$f_l=f_{lr}+if_{li} \quad (l=1,2,3).$$

Here f_2 and f_3 correspond to the higher-order terms. Further, if we set

$$f_1=\epsilon-(b_3-ic_3)|A|^2-(b_5-ic_5)|A|^4,$$

$$f_2=(m_r+im_i)|A|^2,$$

$$f_3=(n_r+in_i)|A|^2,$$

where b, c, m, and n are real constants, then Eq. (1) becomes as follows:

$$\partial_t A=\epsilon A+(b_1+ic_1)\partial_x^2 A-(b_3-ic_3)|A|^2A-(b_5-ic_5)|A|^4A+(m_r+im_i)\partial_x(|A|^2A)+(n_r+in_i)\partial_x(|A|^2)A. \quad (2)$$

If the last two terms on the right-hand side are neglected, Eq. (2) reduce to CGLE, whose dynamical behaviors have extensively been investigated (see, for example, [2,3,19]). However, there is little corresponding study in the presence of the higher-order terms f_2 and f_3. Noting that the model parameters are generally dependent on the selected physical systems. For propagation of nonlinear light pulses in optical systems, $A(z,t)$ is the complex envelope of the electric field, t is the normalized propagation distance, and x is the retarded time. $\epsilon>0(<0)$ represents linear gain (loss), c_1 is group velocity dispersion (GVD), c_3 is nonlinear Kerr effect, b_1 describes the effect of spectral limitation due to gain bandwidth-limited amplification and (or) spectral filtering (which are inversely proportional to gain and (or) spectral filtering bandwidth, respectively), b_3 accounts for nonlinear gain [and (or) absorption] processes, b_5 and c_5 describe the saturable effects of nonlinear gain [and (or) absorption] and nonlinear refractive index, m_r is the nonlinear dispersion term, n_r and n_i are the nonlinear gradient term which results from the time-retarded induced Raman process. In fact, n_i is usually responsible for the SFS. Usually, m_i and n_r are neglected in optical transmission systems because they are much smaller than m_r and n_i.

Similar to Ref. [2], we separate $A(x,t)$ into the following uniformly translating profiles:

$$A(x,t)=e^{-i\omega t}a(\xi)e^{i\phi(\xi)},$$

where $\xi=x-vt$. Inserting this ansatz into Eq. (2) and introducing

$$q=\partial_\xi\phi, \quad k=a^{-1}\partial_\xi a,$$

we get three ordinary differential equations (ODE) in the forms

$$\partial_\xi a=ka, \quad (3a)$$

$$\partial_\xi q=Q, \quad (3b)$$

$$\partial_\xi k=K, \quad (3c)$$

with $Q=Q_0+Q_1$, $K=K_0+K_1$, where

$$Q_0=-\tilde{b}_1(\omega+vq)+\tilde{c}_1(\epsilon+vk)-2kq-(\tilde{b}_1c_3+\tilde{c}_1b_3)a^2-(\tilde{b}_1c_5+\tilde{c}_1b_5)a^4$$

and

$$K_0=-\tilde{c}_1(\omega+vq)-\tilde{b}_1(\epsilon+vk)+q^2-k^2+(\tilde{b}_1b_3-\tilde{c}_1c_3)a^2+(\tilde{b}_1b_5-\tilde{c}_1c_5)a^4,$$

which result from the part of CGLE given by Ref. [2], and K_1 and Q_1 are presented by the new higher-order terms, which can be written by

$$Q_1=2\tilde{c}_1(m_r+n_r)ka^2+\tilde{c}_1m_rka^2-\tilde{b}_1m_rqa^2-2\tilde{b}_1n_ika^2-\tilde{c}_1m_iqa^2-3\tilde{b}_1m_ia^2k,$$

$$K_1=-2\tilde{b}_1(m_r+n_r)ka^2-\tilde{b}_1m_rka^2-\tilde{c}_1m_rqa^2-2\tilde{c}_1n_ika^2+\tilde{b}_1m_iqa^2-3\tilde{c}_1m_ia^2k,$$

where $\tilde{b}_1=b_1(c_1^2+b_1^2)^{-1}$, $\tilde{c}_1=c_1(c_1^2+b_1^2)^{-1}$.

Obviously, for the case of CGLE namely when the higher-order terms are omitted ($Q_1=K_1=0$), the ODE has the symmetry under the following transformation:

$$v\to -v, \quad \xi\to -\xi, \quad k\to -k, \quad q\to -q, \quad a\to -a.$$

However, in the presence of higher-order terms this symmetry cannot be kept because of the asymmetry of Q_1 and K_1.

Corresponding to uniformly translating solutions of the Eq. (2), there are two classes of fixed points in the three variable dynamical system (3). They are so-called ''nonlinear'' fixed points (N) with $a_N\neq 0$, $q_N\neq 0$, $k_N=0$, and ''linear'' ones (L) with $a_L=0$, $q_L\neq 0$, and $k_L\neq 0$. The linear fixed-point solutions with $k_L>0$ ($k_L<0$) can be denoted by $L_+(L_-)$. Besides the fixed points N and L, there exist so-called ''coherent structures'' which are uniformly translating solutions of Eq. (2) with spatially varying envelopes. These coherent structures correspond to (heteroclinic) trajectories of Eq. (3) joining different fixed points, which have been distinguished from three types of coherent structures [2]: pulses going from L_+ to L_-; fronts going from N to L_- (or L_+ to N); and domain walls which join different N fixed points. In the following we will concentrate on discussing the characteristics of the front solution for the higher-order CGLE (2).

We make the following ansatz [2] for a front solution of Eq. (2):

$$q(a^2)=q_N+e_0(a^2-a_N^2), \quad (4a)$$

$$k(a^2)=e_1(a^2-a_N^2), \tag{4b}$$

with constants q_N, a_N, e_0, e_1 to be determined. By inserting the ansatz into the three ordinary differential equations (3) and setting the coefficients of two quadratic polynomial equations equal to zero, we find six relations among the parameters q_N, a_N, e_0, e_1, ω, and v:

$$\omega=\omega^+=-vq+c_1q_N^2-c_3a_N^2-c_5a_N^4-m_rq_Na_N^2, \tag{5a}$$

$$\epsilon=b_1q_N^2+b_3a_N^2+b_5a_N^4+m_iq_Na_N^2, \tag{5b}$$

$$3e_1^2-e_0^2=\tilde{b}_1b_5-\tilde{c}_1c_5-3e_1(m_r\tilde{b}_1+m_i\tilde{c}_1) -2e_1(n_r\tilde{b}_1+n_i\tilde{c}_1)-e_0(m_r\tilde{c}_1-m_i\tilde{b}_1), \tag{5c}$$

$$4e_1e_0=-\tilde{c}_1b_5-\tilde{b}_1c_5-e_0m_r\tilde{b}_1+3e_1m_r\tilde{c}_1+2e_1n_r\tilde{c}_1 -2e_1n_i\tilde{b}_1-3e_1m_i\tilde{b}_1-e_0m_i\tilde{c}_1, \tag{5d}$$

$$0=\tilde{b}_1c_3+\tilde{c}_1b_3-(\tilde{c}_1e_1-\tilde{b}_1e_0)v+2q_Ne_1-6e_0e_1a_N^2 -a_N^2e_0m_r\tilde{b}+m_rq_N\tilde{b}_1+3a_N^2e_1m_r\tilde{c}_1+2a_N^2e_1n_r\tilde{c}_1 -3a_N^2e_1m_i\tilde{b}_1-a_N^2e_0m_i\tilde{c}_1-m_iq_N\tilde{c}_1-2a_N^2e_1n_i\tilde{b}_1, \tag{5e}$$

$$0=\tilde{c}_1c_3-\tilde{b}_1b_3+(\tilde{b}_1e_1+\tilde{c}_1e_0)v-2q_Ne_0+(2e_0^2-4e_1^2)a_N^2 -3a_N^2e_1m_r\tilde{b}_1-3a_N^2e_1n_r\tilde{b}_1-a_N^2e_0e_1m_r+m_rq_N\tilde{c}_1 -2a_N^2e_1n_i\tilde{c}_1+a_N^2e_0m_i\tilde{b}_1-m_iq_N\tilde{b}_1-3a_N^2e_1m_i\tilde{c}_1. \tag{5f}$$

After some algebraic calculation, the front parameters $q_N^+, v^+, (a_N^2)^+, \omega^+$ can be rewritten in an explicit form

$$q_N=q_N^+=e_2+e_3a_N^2, \tag{6a}$$

$$v=v^+=e_4+e_5a_N^2, \tag{6b}$$

$$a_N^4+e_6a_N^2+e_7=0, \tag{6c}$$

$$k_L=k_L^+=-e_1a_N^2, \tag{6d}$$

$$\omega=\omega^+=-vq+c_1q_N^2-c_3a_N^2-c_5a_N^4-m_rq_Na_N^2, \tag{6e}$$

with

$$e_2=\frac{-(\tilde{b}_1^2+\tilde{c}_1^2)(b_3e_0+c_3e_1)}{2\tilde{b}_1(e_0^2+e_1^2)+e_1m_r(\tilde{b}_1^2+\tilde{c}_1^2)+e_0m_i(\tilde{b}_1^2+\tilde{c}_1^2)},$$

$$e_3=\frac{2(e_0^2+e_1^2)(e_0\tilde{b}_1+2e_1\tilde{c}_1)-[2e_0e_1(m_r+n_r)-2e_1^2n_i-m_i(e_0^2+3e_1^2)](\tilde{b}_1^2+\tilde{c}_1^2)}{2\tilde{b}_1(e_0^2+e_1^2)+e_1m_r(\tilde{b}_1^2+\tilde{c}_1^2)+e_0m_i(\tilde{b}_1^2+\tilde{c}_1^2)},$$

$$e_4=\frac{-2e_0(c_3\tilde{b}_1+b_3\tilde{c}_1)+2e_1(b_3\tilde{b}_1-c_3\tilde{c}_1)+b_3m_r(\tilde{b}_1^2+\tilde{c}_1^2)-c_3m_i(\tilde{b}_1^2+\tilde{c}_1^2)}{2\tilde{b}_1(e_0^2+e_1^2)+e_1m_r(\tilde{b}_1^2+\tilde{c}_1^2)+e_0m_i(\tilde{b}_1^2+\tilde{c}_1^2)},$$

$$e_5=\frac{8e_1(e_0^2+e_1^2)+(3e_1m_r+2e_1m_rn_r+3e_1m_i^2+2e_1m_in_i)(\tilde{b}_1^2+\tilde{c}_1^2)}{2\tilde{b}_1(e_0^2+e_1^2)+e_1m_r(\tilde{b}_1^2+\tilde{c}_1^2)+e_0m_i(\tilde{b}_1^2+\tilde{c}_1^2)} +\frac{(e_1^2\tilde{b}_1-e_0e_1\tilde{c}_1)(10m_r+4n_r)+(4e_1n_i+10e_1m_i)(e_0\tilde{b}_1+e_1\tilde{c}_1)}{2\tilde{b}_1(e_0^2+e_1^2)+e_1m_r(\tilde{b}_1^2+\tilde{c}_1^2)+e_0m_i(\tilde{b}_1^2+\tilde{c}_1^2)},$$

$$e_6=\frac{2e_2e_3+\dfrac{b_3}{b_1}}{e_3^2+\dfrac{b_5}{b_1}},$$

$$e_7=\frac{e_2^2-\dfrac{\epsilon}{b_1}}{e_3^2+\dfrac{b_5}{b_1}},$$

and the other two parameters e_0, e_1 can be determined from Eqs. (5c) and (5d). For the parameter e_1 we find that it has to satisfy

$$ae_1^4+be_1^3+ce_1^2+de_1+e=0 \tag{7}$$

with:

$$a=-48,$$

$$b=-72m_r\tilde{b}_1-32n_r\tilde{b}_1-72m_i\tilde{c}_1-32n_i\tilde{c}_1,$$

$$c=16b_5\tilde{b}_1-3m_i^2\tilde{b}_1^2-27m_r^2\tilde{b}_1^2+4m_in_i\tilde{b}_1^2+4n_i^2\tilde{b}_1^2-16m_rn_r\tilde{b}_1^2-16c_5\tilde{c}_1-48m_im_r\tilde{b}_1\tilde{c}_1-20m_rn_i\tilde{b}_1\tilde{c}_1-20m_in_r\tilde{b}_1\tilde{c}_1-8n_in_r\tilde{b}_1\tilde{c}_1-27m_i^2\tilde{c}_1^2-3m_r^2\tilde{c}_1^2-16m_in_i\tilde{c}_1^2+4m_rn_r\tilde{c}_1^2+4n_r^2\tilde{c}_1^2,$$

$$d=2c_5m_i\tilde{b}_1^2+8b_5m_r\tilde{b}_1^2+4c_5n_i\tilde{b}_1^2-3m_i^2m_r\tilde{b}_1^3-3m_r^3\tilde{b}_1^3-2m_im_rn_i\tilde{b}_1^3-2m_r^2n_r\tilde{b}_1^3+10b_5m_i\tilde{b}_1\tilde{c}_1-10c_5m_r\tilde{b}_1\tilde{c}_1+4b_5n_i\tilde{b}_1\tilde{c}_1-4c_5n_r\tilde{b}_1\tilde{c}_1-3m_i^3\tilde{b}_1^2\tilde{c}_1-3m_im_r^2\tilde{b}_1^2\tilde{c}_1-2m_i^2n_i\tilde{b}_1^2\tilde{c}_1-2m_im_rn_r\tilde{b}_1^2\tilde{c}_1-8c_5m_i\tilde{c}_1^2-2b_5m_r\tilde{c}_1^2-4b_5n_r\tilde{c}_1^2-3m_i^3m_r\tilde{b}_1^2\tilde{c}_1-3m_r^3\tilde{b}_1\tilde{c}_1^2-2m_im_rn_i\tilde{b}_1\tilde{c}_1^2-2m_r^2n_r\tilde{b}_1\tilde{c}_1^2-3m_i^3\tilde{c}_1^3-3m_im_r^2\tilde{c}_1^3-2m_i^2n_i\tilde{c}_1^3-2m_im_rn_r\tilde{c}_1^3,$$

$$e=c_5^2\tilde{b}_1^2-c_5m_im_r\tilde{b}_1^3+b_5m_r^2\tilde{b}_1^3+2b_5c_5\tilde{b}_1\tilde{c}_1-c_5m_i^2\tilde{b}_1^2\tilde{c}_1+b_5m_im_r\tilde{b}_1^2\tilde{c}_1+b_5^2\tilde{c}_1^2-c_5m_im_r\tilde{b}_1\tilde{c}_1^2+b_5m_r^2\tilde{b}_1\tilde{c}_1^2-c_5m_i^2\tilde{c}_1^3+b_5m_im_r\tilde{c}_1^3.$$

Then the parameter e_0 can easily be determined by substituting the value of e_1 into Eq. (5d).

From the coefficient expressions of parameter e_1 we see clearly that the coefficients b and d are only related with the higher-order terms. It means that Eq. (7) have single positive root in the case of CGLE. The corresponding negative one only leads to an equivalent front because of the symmetry mentioned above. However, in the presence of higher-order effects Eq. (7) may exist four real roots as the symmetry is broken. Therefore, the higher-order effects will lead to more front solutions, which are dependent strongly on the system parameters.

III. STABILITY ANALYSIS AND NUMERICAL RESULTS

As mentioned by Saarloos [2,3], the condition for existence of a heteroclinic trajectory is that the stable and unstable manifolds of the fixed points in question should join up. It is thus possible to determine the multiplicity of the aforementioned coherent structures by studying the linear stability of the fixed points in the dynamical system of Eq. (3).

The linear stability of the N fixed point in the original partial differential equation (PDE) shown by Eq. (2) can be obtained by the standard linearization. Let

$$A(x,t)=\tilde{a}(x,t)e^{i\tilde{\phi}(x,t)},$$

then the amplitude and phase satisfy the following two PDEs:

$$\partial_t\tilde{a}=\epsilon\tilde{a}+b_1[\partial_x^2\tilde{a}-\tilde{a}(\partial_x\tilde{\phi})^2]-c_1[2(\partial_x\tilde{a})(\partial_x\tilde{\phi})+\tilde{a}\partial_x^2\tilde{\phi}]-b_3\tilde{a}^3-b_5\tilde{a}^5+(3m_r+2n_r)\tilde{a}^2\partial_x\tilde{a}-m_ia^3\partial_x\tilde{\phi}, \quad (8a)$$

$$\tilde{a}\partial_t\tilde{\phi}=b_1[2(\partial_x\tilde{a})(\partial_x\tilde{\phi})+\tilde{a}\partial_x^2\tilde{\phi}]+c_1[\partial_x^2\tilde{a}-\tilde{a}(\partial_x\tilde{\phi})^2]+c_3\tilde{a}^3+c_5\tilde{a}^5+(3m_i+2n_i)\tilde{a}^2\partial_x\tilde{a}+m_ra^3\partial_x\tilde{\phi}. \quad (8b)$$

Further introducing

$$\tilde{a}(x,t)=a_N+\tilde{a}_1,$$

$$\tilde{\phi}(x,t)=q_Nx-\omega_Nt+\tilde{\phi}_1,$$

$$\tilde{a}_1=\tilde{a}_{01}\exp[iPx+\lambda t],$$

$$\tilde{\phi}_1=\tilde{\phi}_{01}\exp[iPx+\lambda t],$$

and linearizing Eq. (8) for $\tilde{a}_{01}$ and $\tilde{\phi}_{01}$, we can get the ensuing characteristic equation for λ:

$$\lambda^2+\beta\lambda+\gamma=0 \quad (9)$$

with

$$\beta=2a_N^2b_3+4a_N^4b_5+2b_1P^2+4ic_1Pq_N-3ia_N^2m_rP-ia_N^3m_rP-2ia_N^2n_rP-a_N^2m_iq_N,$$

and

$$\gamma=2a_N^2b_1b_3P^2+4a_N^4b_1b_5P^2-2a_N^2c_1c_3P^2-4a_N^4c_1c_5P^2+b_1^2P^4+c_1^2P^4+4ia_N^2b_3c_1Pq_N+8ia_N^4b_5c_1Pq_N+4ia_N^2b_1c_3Pq_N+8ia_N^4b_1b_5Pq_N-4b_1^2P^2q_N^2-4c_1^2P^2q_N-2ia_N^5b_3m_rP-4ia_N^7b_5m_rP-3a_N^5m_r^2P^2-2a_N^5m_rn_rP^2-3ia_N^2b_1m_rP^3-ia_N^3b_1m_rP^3-2ia_N^3c_1n_iP^3-2ia_N^2b_1n_rP^3+6a_N^2c_1m_rP^2q_N-a_N^3c_1m_rP^2q_N-4a_N^3b_1n_iP^2q_N+4a_N^2c_1n_rP^2q_N+6ia_N^3b_1m_rPq_N^2+ia_N^5m_im_rPq_N-a_N^2b_1m_iP^2q_N-2ia_N^2c_1m_iPq_N^2.$$

For stability we have to require that the solutions $\lambda(P)$ of Eq. (9) satisfy

$$\mathrm{Re}\,\lambda(P)<0 \quad (10)$$

for all P. Applying this condition for $P\to 0$, we get the necessary stability condition

$$4a_N^2b_5+2b_3-m_iq_N>0 \quad (11)$$

for amplitude perturbations. From this one can easily evaluate $\lambda(P)$ numerically and check the stability of any particular solution a_N, q_N for given parameters.

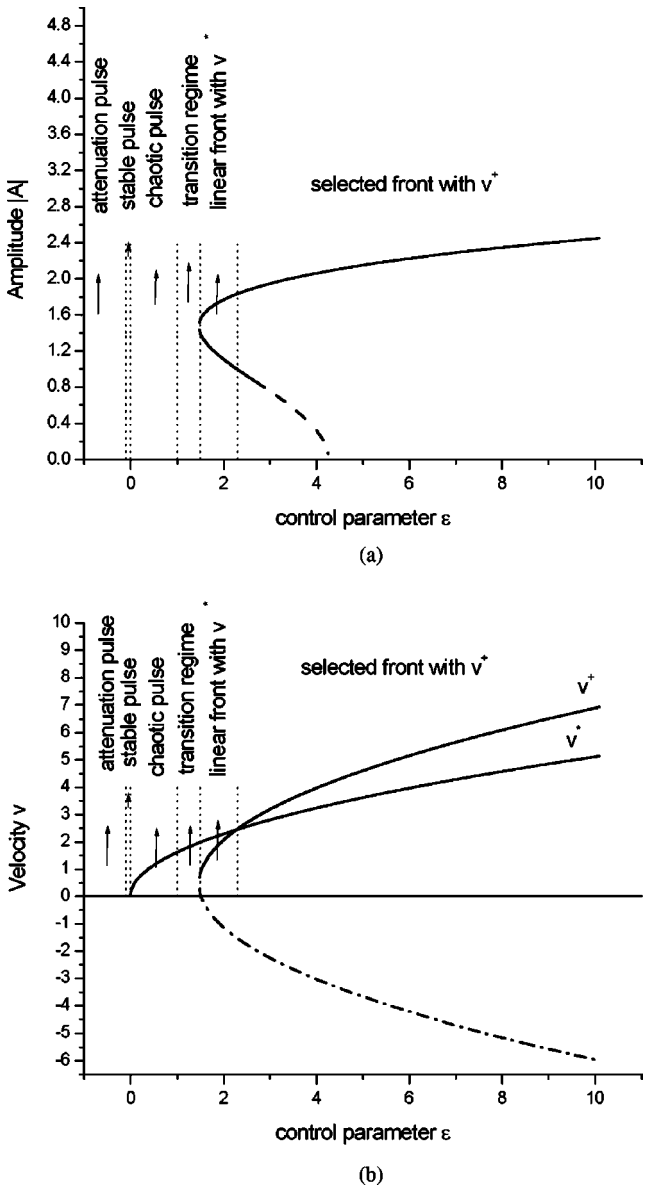

FIG. 1. (a) Bifurcation diagrams (a_n as a function of control parameter ϵ) and the regions for different evolution results when a certain initial condition is given. The parameter values other than those for ϵ are chosen as $b_1=-0.3$, $c_1=0.5$, $b_3=-0.5$, $c_3=1$, $b_5=0.34$, $c_5=0$, $m_r=-0.02$, $m_i=0$, $n_r=0$, $n_i=-0.05$, respectively. (b) Front velocity as a function of control parameter ϵ, where v^* is given by the linear-marginal-stability criterion and v^+ is obtained from Eq. (6b).

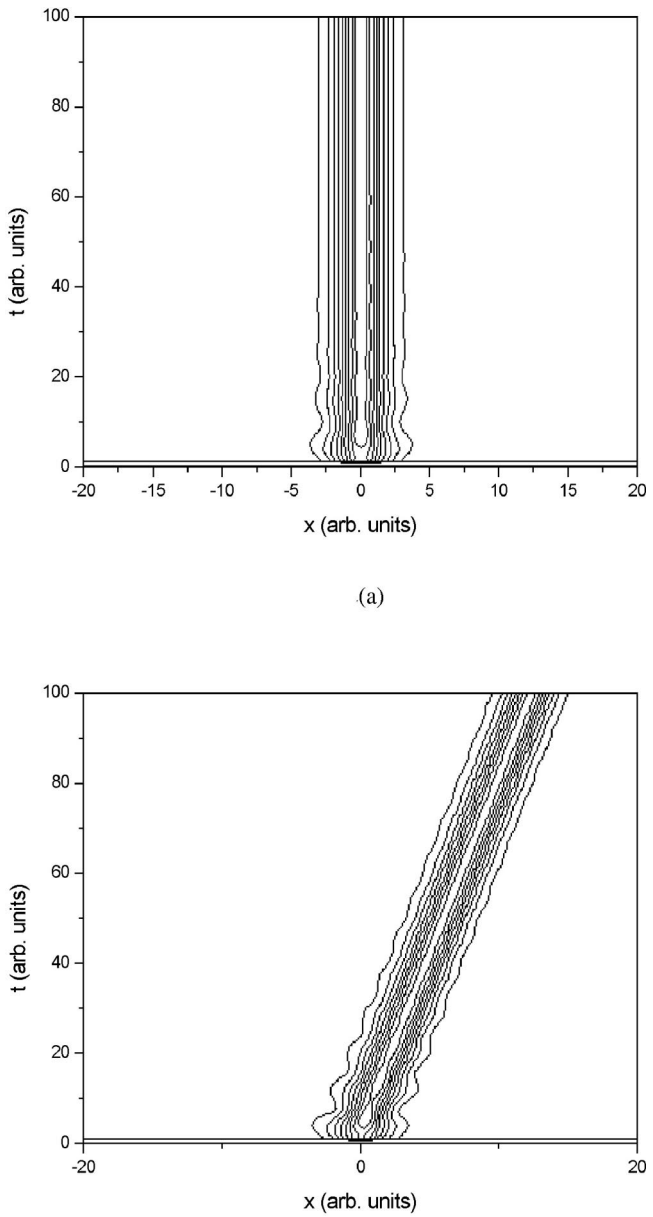

FIG. 2. Contour plots of the stable pulse transmission. The control parameter ϵ is selected as -0.05 and the other parameters are as same as those in Fig. 1. (a) the result when $m_r=0$ and $n_i=0$, namely, the higher-order terms are omitted; (b) the result when the higher-order terms are considered.

The most interesting question about fronts and pulses is their dynamical behavior as solutions of Eq. (2). Now let us investigate the ''selection'' problem of the front solution obtained from the ansatz (4). Here we use the rules developed earlier [2] to elucidate the selection problem. The basic idea is that the selected front v^+,ω^+ is the entity which controls the behavior of the system. From Eq. (6b) we can analytically calculate the parameters v^+ of the selected front. As shown in Ref. [3], when $v^+>0$, a localized initial condition will lead to a positive front described by the solution (4), and pulses will be unstable. In contrast, when $v^+<0$, or when no solution of Eq. (4) exists, the outcome is somewhat more dependent on initial conditions. In such cases, a localized initial condition may lead to an attenuation pulse, or a chaotic pulse. Alternatively, stable stationary pulses may yield for some appropriate parameter range. The latter is of potential applications in optical telecommunication systems. In the following numerical investigations we will concentrate on discussing optical transmission system.

Figure 1 illustrates the different regimes for a set of special parameters as a function of the parameter ϵ. Here we have chosen the values of the parameters from optical trans-

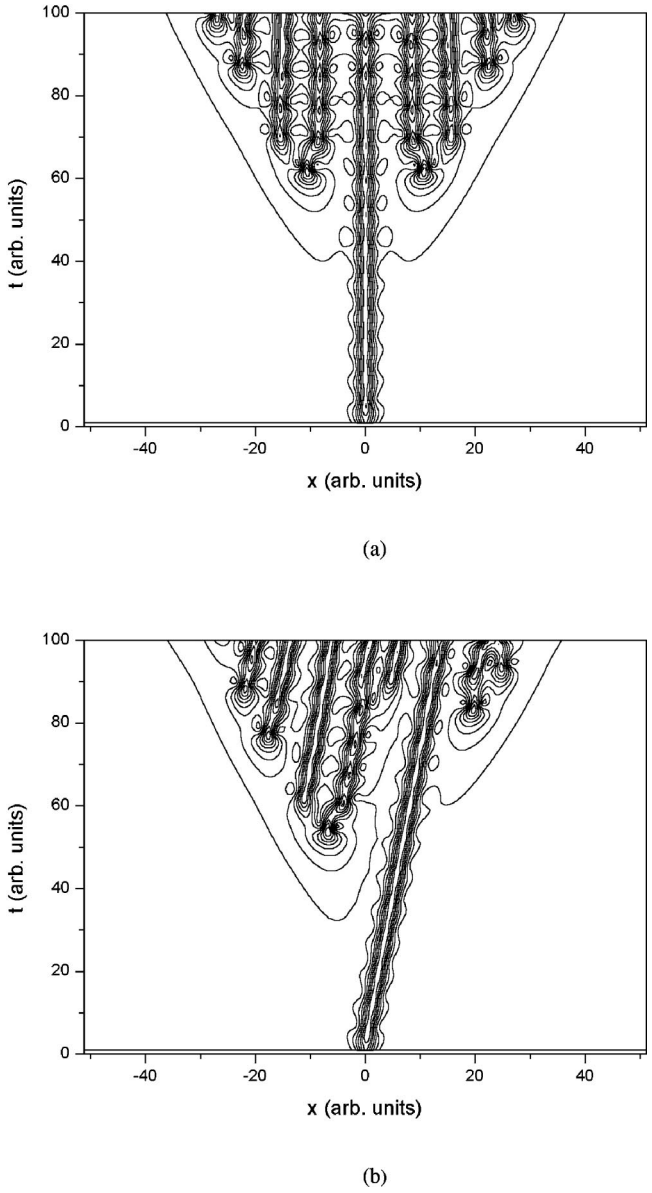

FIG. 3. Contour plots of the chaotic pulse transmission. The control parameter ϵ is selected as 0.05 and the other parameters are as same as those in Fig. 1, (a) the result when $m_r=0$ and $n_i=0$, namely, the higher-order terms are omitted; (b) the result when the higher-order terms are considered.

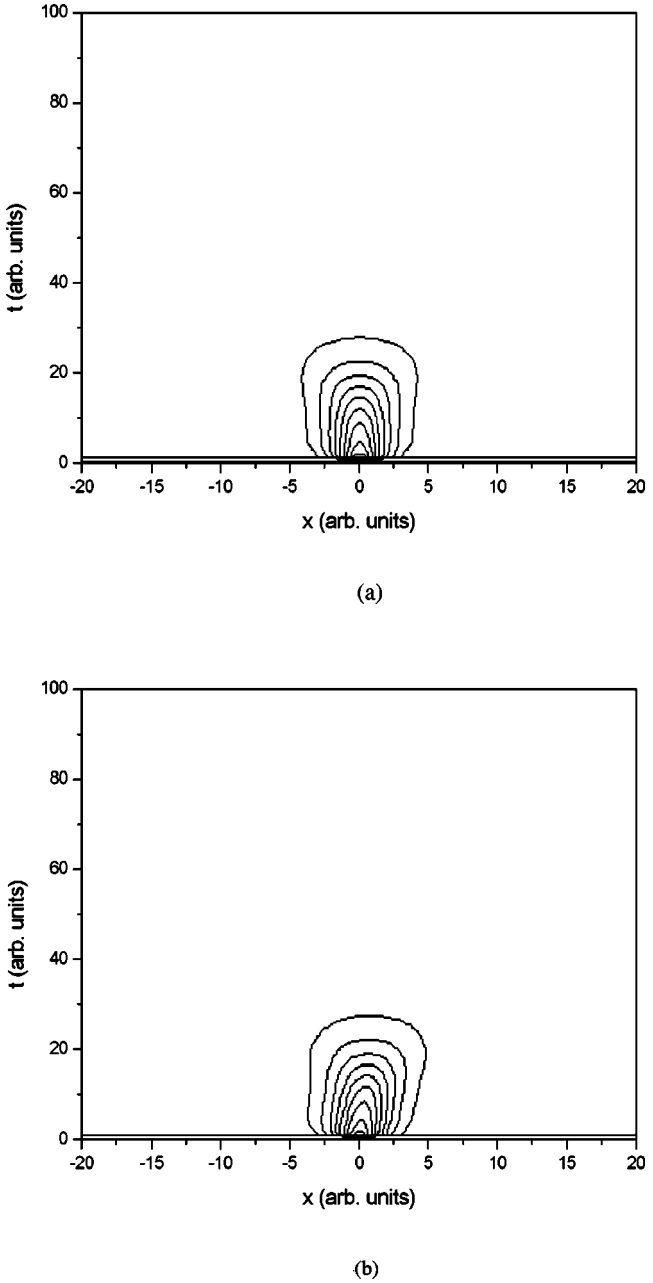

FIG. 4. Contour plots of the attenuation pulse transmission. The control parameter ϵ is selected as -0.09 and the other parameters are as same as those in Fig. 1, (a) the result when $m_r=0$ and $n_i=0$, namely the higher-order terms are omitted; (b) the result when the higher-order terms are considered.

mission systems presented in Refs. [25,27,28]. Figure 1(a) shows the bifurcation diagrams (a_N as a function of control parameter ϵ), where dashed line refers to unstable solutions and solid line refers to stable ones. Figure 1(b) shows the front velocity as a function of the control parameter ϵ, where v^* is given by the linear-marginal-stability criterion [26] and v^+ is obtained from Eq. (6b). From these figures we can clearly see that there exist saddle-node bifurcation, special value bifurcation, and subcritical bifurcation, respectively. The corresponding bifurcation values ϵ are 1.471 64, 2.696 52, and 4.268 17. When the higher-order terms are omitted, these values are 1.304 96, 2.370 49, and 3.845 29 respectively. According to Ref. [3] the selected front velocity is max (v^+, v^*). By calculation, we find that when $1.471\,64\ (1.304\,96) < \epsilon < 2.274\,09\ (1.894\,17)$, the velocity of the front solution (4) satisfies $v^+ < v^*$. Therefore, the linear front will be selected. When $2.274\,09\ (1.89417) < \epsilon < 14.8309\ (8.480\,76)$, the velocity v^+ is larger than the velocity v^* and the front with velocity v^+ is selected. However, for $\epsilon > 14.8309\ (8.480\,76)$, although $v^+ > v^*$ is satisfied, the linear front is still selected because of $|k|^+ < |k|^*$ [2,3]. The values mentioned above in the bracket correspond to the case where the higher-order terms are omitted.

Further, when $\epsilon < 1.47164$ (1.30496), solution (4) does not exist any more. As predicted above, in this case there may exist attenuation pulses, chaotic pulses and stable pulses. By numerical simulation, we found stable pulses in a certain parameter regimes both in the case without higher-order terms and in the case with higher-order terms. The parameter regimes are shown in Fig. 1. The numerical method used here is symmetrized split-step Fourier method [25]. The step size in x direction is 0.1 and the number of discrete points is 1024. The step size in t direction is 1/125. We have checked our results with different step size along the t direction and with different point numbers along the x direction to ensure that the results contain no numerical artifacts. Figure 2(a) plots the contour of stable propagation of optical pulse for given initial condition in the absence of higher-order effects, where $\epsilon = -0.05$. When the higher-order effects exist, as shown in Fig. 2(b), the stable optical pulse has not been destroyed except it moves at a definite speed. The reason is that the symmetry in the case of CGLE cannot be kept when the higher-order terms are not neglected.

Out of the front and the pulse regimes, a localized initial condition may decay to zero or lead to a chaotic pulse. The regimes for the attenuation pulse and chaotic pulse are also shown in Fig. 1, the contours of every kinds of evolution results are shown in Fig. 3 and Fig. 4. As shown in the Fig. 3(a) and 3(b), where the control parameter $\epsilon = 0.05$, Chaotic pulse which started from a stationary localized initial condition has complex shapes. After a while from the beginning, small ripples appeared on its ''slopes,'' then with the ripples' increasing in size, other ripples appeared. At last the ripples can not be distinguished and chaotic pulse come into being. As explained in the stable pulse case, the higher-order terms will lead to moving of the chaotic pulse. And when the value of ε is too small, the attenuation pulses are observed. This is because the loss is too large to keep the propagation of optical pulses. The results are shown in Fig. 4(a) and 4(b), where the control parameter $\epsilon = -0.09$.

IV. CONCLUSION

In conclusion, based on the CGLE with higher-order terms, we have investigated their influences on the multiplicity of solutions and obtained an exact analytic front solution. By linearized stability analysis for the original partial differential equation, we derive its necessary stability condition for amplitude perturbations. This condition together with the exact front solution determines the region of parameter space where the uniformly translating front solution can exist. If the control parameter ϵ is out of the range, stable pulses, chaotic pulses, and attenuation pulses appear generally, which are greatly dependent on the localized initial conditions. We have applied these analysis into the optical transmission system and found the stable evolution of optical pulses by solving partial differential equation numerically. The numerical results are in agreement with the analytic predictions. The higher-order effects will mainly break the symmetry in the case of CGLE and result in moving of the optical pulses. It may be expectable to apply these results into high-capacity optical telecommunications.

ACKNOWLEDGMENTS

This research was supported by National Natural Science Foundation of China Grant No. 10074041 and the Shanxi Province Youth Science Foundation (Grant No. 20011015).

[1] John Guckenheimer and Philip Holmes, *Nonlinear Oscillations, Dynamical Systems, and Bifurcations of Vector Fields*, Applied Mathematical Sciences Vol. 42 (Springer-Verlag, Belin, 1997).
[2] W. van Saarloos, Phys. Rev. A **37**, 211 (1988); **39**, 6367 (1989); W. van Saarloos and P. C. Hohenberg, Physica D **56**, 303 (1992), and reference therein.
[3] W. van Saarloos and P. C. Hohenberg, Phys. Rev. Lett. **64**, 749 (1990).
[4] K. Nozaki and N. Bekki, Phys. Rev. Lett. **51**, 2171 (1983); N. Bekki and K. Nozaki, Phys. Lett. **110A**, 133 (1985).
[5] J. J. Hegseth, C. D. Andereck, F. Hayot, and Y. Pomeau, Phys. Rev. Lett. **62**, 257 (1989).
[6] G. Ahlers and D. S. Cannell, Phys. Rev. Lett. **50**, 1583 (1983).
[7] M. Niklas, M. Lücke, and H. Müller-Krumbhaar, Phys. Rev. A **40**, 493 (1989).
[8] J. Wu, R. Keolian, and I. Rudnick, Phys. Rev. Lett. **59**, 2744 (1987); S. Douady, J. Fluid Mech. **221**, 383 (1990).
[9] M. J. Landman, Stud. Appl. Math. **76**, 187 (1987).
[10] A. Hasegawa, *Optical Solitons in Fibers* (Springer, New York, 1989).
[11] J. V. Moloney and A. C. Newell, Physica D **44**, 1 (1990).
[12] G. S. Skinner and H. L. Swinney, Physica D **48**, 1 (1991).
[13] L. C. Crasovan, B. A. Malomed, D. Mihalache, D. Mazilu, and F. Lederer, Phys. Rev. E **62**, 1322 (2000), and reference therein.
[14] P. Kolodner, Phys. Rev. A **44**, 6448 (1991).
[15] K. J. Blow, N. J. Dorran, and D. Wood, J. Opt. Soc. Am. B **5**, 381 (1988).
[16] P. A. Bėlanger, L. Gagnon, and C. Parė, Opt. Lett. **14**, 943 (1989).
[17] Y. Chen, Electron. Lett. **27**, 1985 (1991).
[18] G. P. Agrawal, Phys. Rev. A **44**, 7493 (1991).
[19] M. C. Cross and P. C. Hohenberg, Rev. Mod. Phys. **65**, 851 (1993).
[20] B. I. Shraiman, A. Pumir, W. van Saarloos, P. C. Hohenberg, H. Chatė, and M. Holen, Physica D **57**, 241 (1992); P. J. Aston and C. R. Laing, *ibid.* **135**, 79 (2000); H. Sakaguchi and B. A. Malomed, *ibid.* **147**, 273 (2000).
[21] M. van Hecke, Phys. Rev. Lett. **80**, 1896 (1998).
[22] L. Brusch, M. G. Zimmermann, M. van Hecke, M. Bar, and A. Torcini, Phys. Rev. Lett. **85**, 86 (2000).
[23] M. van Hecke and M. Howard, Phys. Rev. Lett. **86**, 2018 (2001).

[24] R. J. Deissler and H. R. Brand, Phys. Rev. Lett. **81**, 3856 (1998).
[25] See, for example, G. P. Agrawal, *Nonlinear Fiber Optics* (Academic Press, New York, 1995).
[26] G. Dee and J. S. Langer, Phys. Rev. Lett. **50**, 383 (1983).
[27] M. Matsumoto, H. Ikeda, T. Uda, and A. Hasegawa, J. Lightwave Technol. **13**, 658 (1995).
[28] L. Gagnon and P. A. Bèlanger, Phys. Rev. A **43**, 6187 (1991).